

Seasonal variation of chlorophyll and primary productivity in central Arabian Sea: A macrocalibrated upper ocean ecosystem model

M K SHARADA and K S YAJNIK*

CSIR Centre for Mathematical Modelling and Computer Simulation (C-MMACS), Bangalore 560 037, India

*Present address: Regal Manor, 2/1 Bride Street, Langford Town, Bangalore 560 025, India;
email: ksy@letterbox.com

Seasonal variation of chlorophyll has been of considerable interest on account of the effect of photosynthesis on ocean-atmosphere carbon exchange. It can be predicted by a dynamical system model of the marine ecosystem coupled with a physical oceanographic model. There is however a major difficulty in the calibration of contemporary ecosystem models on account of sparse data and a large number of model parameters. This paper reports a new approach of macrocalibration in which values of six parameters are determined by examining in detail the seasonal variation of chlorophyll and primary productivity keeping in view the observations of two Indian JGOFS cruises. Both switching and non-switching versions of grazing functions are used in a 7-component FDM model. Detailed simulations are reported for one station (16°N, 65°E). They show the effects of dependence of grazing preference on prey density on the behaviour of the ecosystem. The results of the simulation also provide a partial basis for developing correlations of primary production with chlorophyll and sediment flux.

1. Introduction

The response of the marine ecosystem in the upper ocean is of interest from several viewpoints. The biological pump transfers a considerable amount of carbon from the euphotic zone to the deep ocean as organic matter, the basic mechanism being fixation of inorganic carbon into organic molecules during photosynthesis (Sathyendranath and Platt 1994). Also, the available fish catch depends on the response of the marine ecosystem to environmental factors like nutrients, photosynthetically active radiation etc., (Wroblewski *et al* 1989). Furthermore, biological processes in the surface layer influence the net transport of heat by the ocean (Sathyendranath *et al* 1991). Also, the plankton produce volatile organic compounds such as dimethyl sulphide which help in the formation of clouds (Jonathan *et al* 1991).

Ocean carbon cycle models coupled with ocean-atmosphere general circulation models, can describe

the long-term response of the ocean system to global change scenarios. As a first step towards the development of such coupled basin-scale models of ocean circulation and biogeochemical cycles, we have been studying at C-MMACS a class of dynamical models of marine ecosystems (Yajnik and Sharada 1992). We examine this class of models in the context of the Arabian Sea. Curiously enough, we do not know at present whether the Arabian Sea is a net source or sink of atmospheric carbondioxide (Lal 1994). The principal unique feature of the Arabian Sea conditions is a fairly regular oscillation of high rates of primary production followed by generally oligotrophic conditions under relatively constant levels of illumination (US GLOBEC Report 1993). These oscillations are driven by large-scale atmospheric circulation. The seasonal variability observed in the Arabian Sea is the largest among all ocean basins (Shetye *et al* 1994). The fair degree of regularity of the reversals in conditions, both in space and time, allows experiments to

Keywords. Chlorophyll; primary productivity; ecosystem model; Arabian Sea; model calibration; marine ecosystem.

study factors controlling primary production, transformation and the vertical flux of carbon and nitrogen in deep-water environments (Banse 1994). The unusual atmospheric forcing of the region also creates areas of high productivity that are adjacent to areas of perennially low primary productivity (US GLOBEC Report 1993). These two contrasting production systems in this region offer opportunities for expanding knowledge of oceanic carbon and nitrogen cycles (Lal 1994). The unique conditions in the Arabian Sea give rise to the highest known rates of primary productivity and greatest rates of water column denitrification that are separated in time and space (US GLOBEC Report 1993). Finally, the link between physical forcing and supply of organic matter to depth is the planktonic food web that has special features in the Arabian Sea (Banse 1994).

2. Marine ecosystem models

The central problem of modelling marine ecosystem is to model the interaction between various components of the ecosystem under conditions determined by environmental factors like solar radiation, mixed layer depth, nutrient supply etc. Various models of increasing complexity and realism have been proposed. As early as 1949, Riley *et al* proposed a simple diffusion model. Later many models were constructed which mainly dealt with plankton-herbivore interactions (Steele 1974; Steele and Frost 1977). The role of nutrients in the growth of plankton has been explicitly incorporated in several models (Evans and Parlow 1985; Frost 1987; Wroblewski *et al* 1988 and Taylor and Joint 1990). Models analysing the spatial distribution have also been extensively studied (Levin 1980). Generally, these models consider three components namely, phytoplankton, zooplankton and nutrients.

Modern models (see Appendix I) have three to eleven components and differ significantly from the earlier models. The most important aspect of these models is that most of them incorporate bacteria in the model to provide an alternate source of nitrogen by recycling. Many of them contain different forms of nitrogen which is assumed to be the limiting nutrient. Some of these models also include carbon chemistry. Some models consider different subdivisions of phytoplankton, zooplankton, dissolved organic nitrogen and detritus based on size or activity.

3. Modelling methodology

We employ two versions of a model due to Fasham, Ducklow and McKelvie in which the populations of phytoplankton and zooplankton are not divided into classes based on size (Fasham *et al* 1990). In the first

version, preferences are independent of prey density. In the second version, dependence on the prey density is included. They are respectively called the non-switching version and the switching version. We deal with both the versions as there is an ongoing debate on whether prey-density dependence should be modelled in grazing by zooplankton and, if so, how. Details are given in Appendix II. Also, since many modelling issues have been discussed at length elsewhere (Fasham *et al* 1993; Sarmiento *et al* 1993), those arguments are not repeated here. Briefly, the model describes the temporal response of the marine ecosystem consisting of seven components, namely, phytoplankton, zooplankton, bacteria, detritus, nitrate, ammonium and dissolved organic nitrogen. The model is intrinsically nonlinear as the growth and grazing terms are nonlinear functions of nutrients, solar radiation and population.

The model is applied here to the top ocean layer, called the mixed layer, where temperature variation with depth is negligible. The general problem is to determine the response of the marine ecosystem in the mixed layer for the given temporal variation of solar radiation, mixed layer depth and subsurface nitrate concentration.

In order to focus attention on biological aspects, we neglect net horizontal advection, as the effect of horizontal advection is generally small away from regions of high horizontal gradients. Furthermore, this effect can be effectively incorporated at a later stage when a tested biological model is coupled with an ocean circulation model. This step, in our opinion, is essential as the number of parameters is so large that the problem of testing a coupled model is intractable without adequate prior testing of the biological model.

We consider typical seasonal variation in the ecosystem by assuming that the environmental factors do not have interannual variability. The periodic environmental forcing is constructed from the annual variation of solar radiation and mixed layer depth from the climatological sources (Rao *et al* 1991) by linearly interpolating monthly averages. All the simulations are subjected to this common forcing.

We report here the results of simulations carried out at a station (16°N, 65°E), which lies close to the north-south track on the first and second cruise of the Indian JGOFS programme and to the northern tip on the north-south segment of US-JGOFS transect. It is also close to the location of an Indo-German sediment trap. This proximity, it is hoped, would help us in the evaluation of the model performance.

However, in order to calculate the response, one has to specify the values of the model parameters. There are two nontrivial difficulties in parameter estimation. One is the acute sparsity of data. The other is the large number of parameters (see Appendix II).

The approach adopted in the present work is as follows: The first step was to conduct a parameter

Table 1. Values of parameters governing nutrient supply.

Group	A	B	C	D
Subsurface nitrogen N_0 (mMol N/cu m)	10	10	20	20
Thermocline mixing parameter m (m/d)	0.1	1.0	0.1	1.0

Table 2. Values of biological parameters.

Case	Asymptotic grazing rate g (/d)	Detritus sinking rate V (m/d)	Grazing preference for phyto- plankton p_1	Grazing preference for bacteria p_2
1	1	1	0.4	0.30
2	1	1	0.5	0.25
3	1	10	0.4	0.30
4	1	10	0.5	0.25
5	2	1	0.4	0.30
6	2	1	0.5	0.25
7	2	10	0.4	0.30
8	2	10	0.5	0.25

sensitivity study for the Arabian Sea with a view to identify major parameters which determine the response in the context of climatic change, that is,

annual/monthly averages of populations, as well as fluxes. We have selected six parameters on the basis of such a study. However, the parameters governing the preference of the zooplankton for the phytoplankton, p_1 , for the bacteria, p_2 , and for detritus, $p_3 = 1 - p_1 - p_2$, were varied by taking two sets of values (0.4, 0.3, 0.3 & 0.5, 0.25, 0.25) to check only one issue, namely, whether a strong preference for phytoplankton is realistic. So we have effectively varied five parameters. The values for the rest were assumed on the basis of available literature. If we view the calibration process as a search and select process, various strategies can be considered for sampling the parameter space. What we consider here is essentially the breadth first strategy in which we search large chunks of the region of interest in the parameter space and exclude those which give unacceptable behaviour. The second stage of the strategy aims at fine tuning the parameters and it may be called microcalibration. Here we have restricted ourselves to the first stage which may be termed as macrocalibration. Furthermore, we selected two values of each parameter so that they roughly sampled the high and the low end of the ranges reported in the literature.

Table 3. Monthly averages of chlorophyll (mg/m^3). Model output for various simulations*.

Group	Case no	Feb.	Mar.	Apr.	May
A	1	0.40 (0.38)	0.46 (0.43)	0.46 (0.42)	0.57 (0.51)
	2	0.35 (0.34)	0.41 (0.40)	0.42 (0.38)	0.47 (0.46)
	3	0.41 (0.37)	0.43 (0.38)	0.49 (0.42)	0.85 (0.70)
	4	0.35 (0.34)	0.37 (0.35)	0.44 (0.40)	0.74 (0.66)
	5	0.18 (0.17)	0.24 (0.21)	0.26 (0.21)	0.42 (0.23)
	6<	0.00 (0.15)	0.59 (0.19)	0.49 (0.18)	0.40 (0.19)
	7	0.19 (0.19)	0.26 (0.21)	0.24 (0.21)	0.30 (0.22)
	8	0.39 (0.16)	0.43 (0.20)	0.26 (0.19)	0.33 (0.20) _v
B	1	0.54 (0.39)	0.65 (0.51)	0.74 (0.42)	0.91 (0.63)
	2<	1.21 (0.33)	1.33 (0.43)	0.67 (0.38)	1.28 (0.56)
	3	0.49 (0.41)	0.90 (0.53)	0.50 (0.44)	0.98 (0.62)
	4<	0.93 (0.36)	1.02 (0.45)	0.72 (0.42)	0.84 (0.52)
	5	0.19 (0.20)	0.29 (0.20)	0.25 (0.24)	0.63 (0.24)
	6<	0.54 (0.15)	0.00 (0.19)	1.12 (0.19)	0.89 (0.19)
	7	0.20 (0.17)	0.30 (0.22)	0.38 (0.23)	0.50 (0.22)
	8<	0.00 (0.16)	0.81 (0.20)	0.72 (0.20)	0.00 (0.20)
C	1	0.48 (0.39)	0.72 (0.49)	0.70 (0.43)	0.54 (0.51)
	2<	0.00 (0.33)	1.87 (0.43)	1.52 (0.39)	1.22 (0.44)
	3	0.50 (0.41)	0.73 (0.51)	0.56 (0.45)	0.62 (0.51)
	4	0.80 (0.35)	0.76 (0.45)	0.45 (0.42)	0.65 (0.46)
	5	0.18 (0.17)	0.25 (0.20)	0.27 (0.21)	0.21 (0.23)
	6<	0.88 (0.15)	0.04 (0.19)	0.82 (0.18)	0.00 (0.19)
	7	0.19 (0.18)	0.27 (0.21)	0.29 (0.22)	0.22 (0.25)
	8<	0.00 (0.16)	0.38 (0.20)	0.71 (0.19)	1.00 (0.20)
D	1	0.37 (0.39)	0.89 (0.51)	0.88 (0.43)	0.86 (0.74)
	2<	2.05 (0.34)	0.03 (0.42)	3.54 (0.43)	2.40 (0.48)
	3<	0.52 (0.41)	0.59 (0.54)	0.62 (0.46)	1.35 (0.78)
	4<	1.36 (0.36)	0.39 (0.44)	1.82 (0.48)	2.40 (0.50)
	5	0.19 (0.16)	0.28 (0.21)	0.25 (0.20)	0.71 (0.21)
	6<	1.51 (0.16)	0.00 (0.20)	1.80 (0.19)	0.00 (0.18)
	7	0.20 (0.17)	0.30 (0.23)	0.26 (0.24)	0.72 (0.19)
	8<	0.00 (0.16)	1.12 (0.20)	0.03 (0.20)	0.96 (0.19)

*Values for second variant given in brackets.

Table 4. *Indian JGOFS data on chlorophyll and primary productivity in the mixed layer at 16°N, 65°E.*

Cruise period	Feb.–Mar.	Apr.–May
Climatological mixed layer depth (m)	60	40
Chlorophyll averaged over the above depth (mg m^{-3})	0.6	0.1
Primary productivity averaged over the above depth ($\text{mg C m}^{-3} \text{d}^{-1}$)	10.2	4.1

The methodology is not altered even if more values are selected for each parameter. The choice of two values was for simplicity. We group 32 simulations obtained by a combination of values of six parameters (effectively five) into four groups. One group differs from another in the supply of nutrients, which depends on the subsurface nitrate, N_0 , and the thermocline mixing parameter, m . The values of these parameters are given in table 1. There are eight cases within each group and they differ in biological

parameters governing grazing and detritus sinking (see table 2).

Since we are interested in climatological studies, we consider monthly and yearly averages of system variables and fluxes. Simulations are carried out for at most six years with a common selected initial condition. On the basis of several numerical experiments, the reported results are believed to be insensitive to the initial conditions that have been used by us. The monthly and yearly averages over the sixth year hardly differ from those in the fourth. Consequently, the averages that are reported here are for the fourth year.

4. Macrocalibration of the model

We now examine the simulations with a view to select one combination of five independent parameters which sample relevant regions in the 5-dimensional parameter subspace. For this purpose we consider the chlorophyll monthly average in Feb.–May (table 3). It is seen that the cases marked with '<' have averages

Table 5. *Monthly averages of primary productivity ($\text{mgC/m}^3/\text{day}$). Model output for various simulations*.*

Group	Case no.	Feb.	Mar.	Apr.	May
A	1<>	16.2 (16.2)	18.8 (19.0)	19.9 (20.0)	25.0 (24.9)
	2<>	13.5 (15.2)	17.4 (19.0)	20.2 (20.2)	25.4 (24.9)
	3	9.3 (8.6)	7.4 (6.7)	6.7 (6.1)	12.6 (12.2)
	4	9.0 (8.3)	7.2 (6.4)	6.6 (6.0)	12.6 (12.2)
	5<	9.1 (8.7)	13.9 (12.1)	18.6 (15.8)	25.0 (19.2)
	6<	0.0 (7.7)	16.9 (11.2)	18.5 (13.8)	18.0 (15.9)
	7	9.5 (9.3)	14.2 (12.1)	15.1 (14.8)	17.4 (17.1)
	8	13.4 (8.3)	12.3 (11.6)	11.1 (13.7)	19.5 (16.2)
B	1<>	21.4 (18.8)	26.3 (28.4)	41.5 (30.7)	46.2 (47.9)
	2<>	29.5 (16.0)	29.9 (25.1)	25.5 (28.1)	39.1 (44.0)
	3<>	20.2 (19.8)	39.7 (30.1)	28.8 (31.7)	52.7 (46.7)
	4<>	25.9 (17.2)	26.6 (26.4)	27.5 (30.7)	39.8 (41.0)
	5<	9.8 (10.2)	16.9 (12.6)	17.9 (18.5)	35.0 (19.5)
	6<	12.1 (7.8)	0.2 (11.9)	28.7 (14.8)	29.5 (16.7)
	7<	10.5 (9.1)	17.5 (14.1)	24.9 (18.0)	28.2 (19.2)
	8<	0.0 (8.4)	21.5 (13.0)	26.8 (15.7)	0.0 (17.5)
C	1<>	20.0 (18.4)	31.0 (26.9)	41.6 (30.6)	37.6 (40.6)
	2<>	0.0 (16.0)	36.6 (24.1)	36.8 (28.5)	36.9 (36.4)
	3<>	20.8 (19.3)	31.7 (27.8)	30.3 (30.5)	38.9 (37.2)
	4<>	20.7 (17.0)	22.1 (25.3)	19.2 (29.3)	34.4 (34.9)
	5<	9.2 (8.9)	14.4 (12.1)	20.1 (15.9)	15.5 (19.8)
	6<	20.4 (7.7)	1.6 (11.4)	30.7 (14.0)	0.0 (16.1)
	7<>	10.0 (9.4)	15.8 (13.0)	21.7 (17.2)	16.0 (21.3)
	8<	0.2 (8.3)	13.3 (12.4)	18.4 (15.1)	35.7 (17.3)
D	1<>	15.6 (19.0)	36.2 (28.9)	48.6 (31.4)	47.9 (55.4)
	2<>	33.3 (16.2)	2.2 (24.5)	61.9 (31.9)	56.3 (40.0)
	3<>	20.9 (20.0)	29.0 (30.6)	36.4 (33.7)	74.0 (57.5)
	4<>	28.0 (17.4)	9.9 (26.0)	53.0 (36.0)	62.9 (40.2)
	5<	9.7 (8.2)	16.9 (13.2)	17.5 (16.1)	40.6 (18.3)
	6<	31.8 (8.3)	0.0 (12.3)	46.9 (15.2)	0.0 (16.0)
	7<	10.6 (9.3)	18.4 (14.7)	18.3 (19.1)	41.0 (17.0)
	8<	0.1 (8.4)	26.5 (13.0)	2.4 (15.9)	32.6 (17.7)

* Values for the second variant are given in brackets in both tables 3 and 5.

< indicates unrealistic behaviour for the first variant of the model.

> indicates unrealistic behaviour for the second variant of the model in both tables 3 and 5.

Table 6. Selected parameter values.

Parameter	m	N_0	g	V	p_1	p_2
Selected value	0.1	10	2	10	0.4	0.3

obtained with the non-switching version which are rather high ($> 1 \text{ mg/m}^3$) or low ($< 0.01 \text{ mg/m}^3$). These values are regarded as unrealistic in view of the estimates based on the JGOFS data given in table 4.

The data in table 4 are somewhat like snapshot values, while the model results are for monthly averages. Also, the above results correspond to the years 1994 and 1995, while the model results are for seasonal variations under climatological conditions. Despite these differences, it seems reasonable to rule out the cases marked with '<' as unrealistic, since a generous margin is used for rejecting very high or very low values.

We notice that while some even numbered cases (corresponding to marked preference for phytoplankton) give unrealistic chlorophyll values for the non-switching version, all the cases for the switching version are within acceptable range of chlorophyll. It is also observed that while the non-switching variant gives rise to marked oscillations in chlorophyll values (e.g., C6), the switching variant is free from this feature. If we compare the chlorophyll values for the cases 5 and 7 of the four groups in either of the two versions, we find that the effect of the detritus sinking rate is rather small.

Table 5 gives values of primary productivity from Feb. to May for all the simulations. Here also arrows (<, >) indicate rather high values ($> 20 \text{ mgC/m}^3/\text{day}$) or rather low ($> 0.20 \text{ mgC/m}^3/\text{day}$) in the non-switching and switching versions. We assess these results as unrealistic in view of the Indian JGOFS cruise data (table 4).

We observe that all the first four cases in groups B, C and D give unrealistic productivity in either of the two versions of the model. These cases correspond to $g = 1/\text{day}$. If we examine the results of tables 3 and 5 together, we find that 50% or more of the cases in B, C and D are unrealistic.

In order to be able to compare the behaviour of the two versions, it is necessary to select a common set of values of the calibration parameters. In view of the above arguments, we select the values given in table 6, which correspond to the case A7.

5. Results

The ecosystem model is driven by the subsurface nitrate, which is assumed to be a constant, and the solar radiation and the mixed layer depth, whose seasonal variation is shown in figure 1. Rapid deepening of the mixed layer during the summer

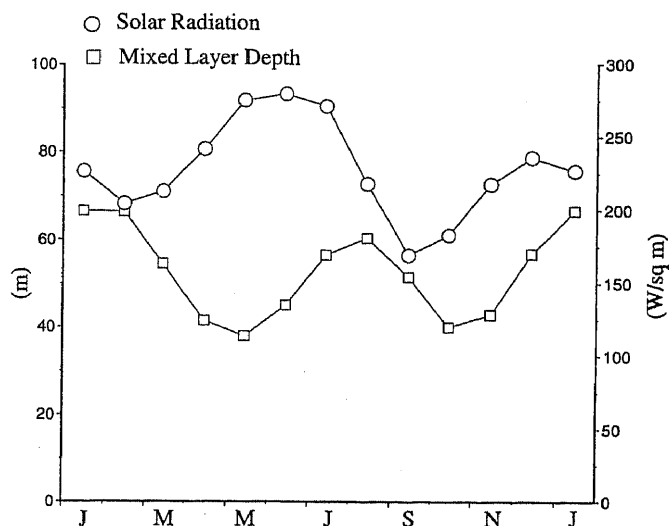


Figure 1. Seasonal variation of mixed layer depth and solar radiation at 16°N , 65°E used as a periodic input for the simulation.

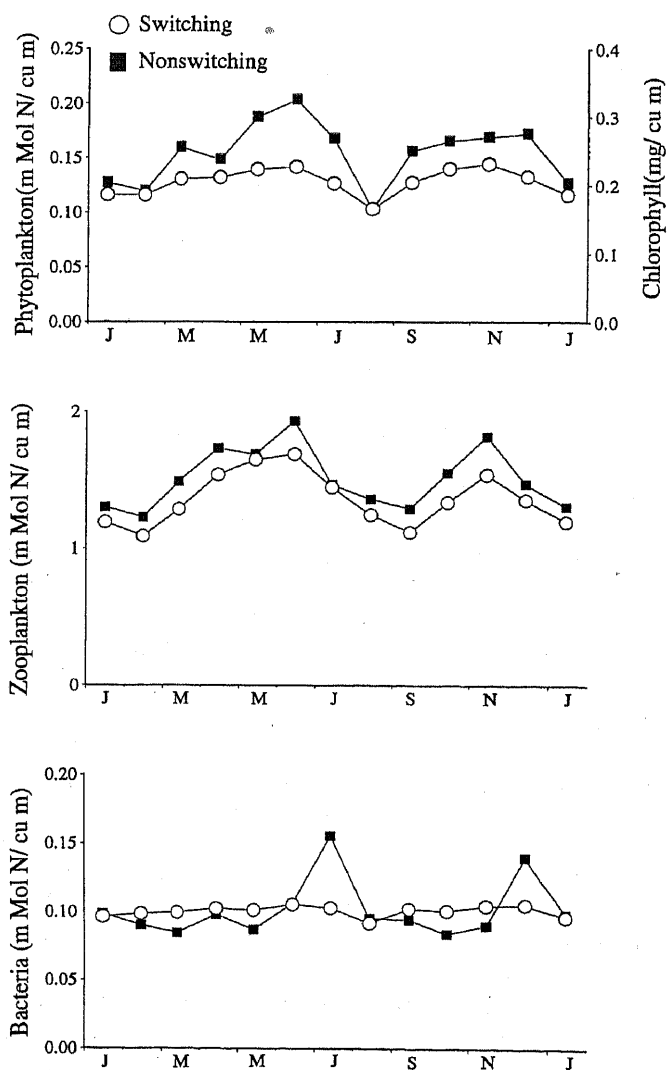


Figure 2. Monthly averages of phytoplankton/chlorophyll, zooplankton and bacteria obtained by the simulation for 16°N , 65°E .

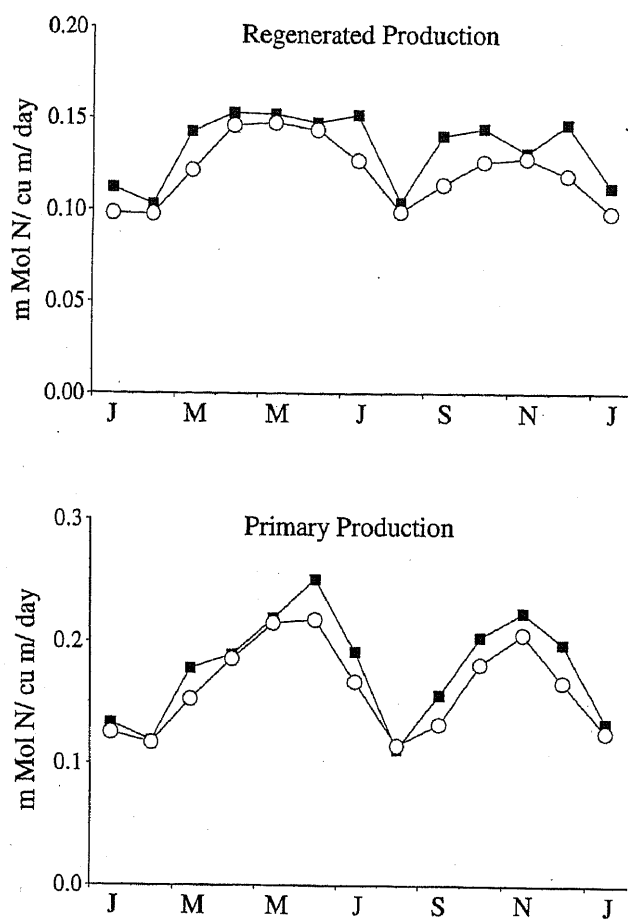


Figure 3. Seasonal variation of primary production and regenerated production.

season and during the winter season brings in considerable nitrates from below, and results in two sharp peaks in nitrate flux. Monthly averages of chlorophyll, zooplankton and bacteria (figure 2) show two peaks in the non-switching version, but the phytoplankton peaks are significantly broader. (Also, there is a third small peak in winter in the non-switching version.) This is due to the large contribution of regenerated production in the total primary production (figure 3) in both the versions. The switching version however flattens out these peaks markedly. In fact, there is hardly any variation in the population of bacteria. It is noted that in both the versions, zooplankton contributes a large fraction of the total biomass as the zooplankton grazes not only on phytoplankton but also on bacteria and on detritus with relative preferences of 0.4, 0.3 and 0.3. Since this type of relative abundance is not observed in temperate seas, it could be a distinguishing feature of the ecosystem in the tropical seas.

The seasonal variation of new production and f-ratio (figure 4), shows peaks which are sharper for the first version. The peaks occur in June and November on account of the rate of deepening of the mixed layer and also decrease in nitrate within the mixed layer. It may be noted that f-ratio is less than 0.5 in all seasons.

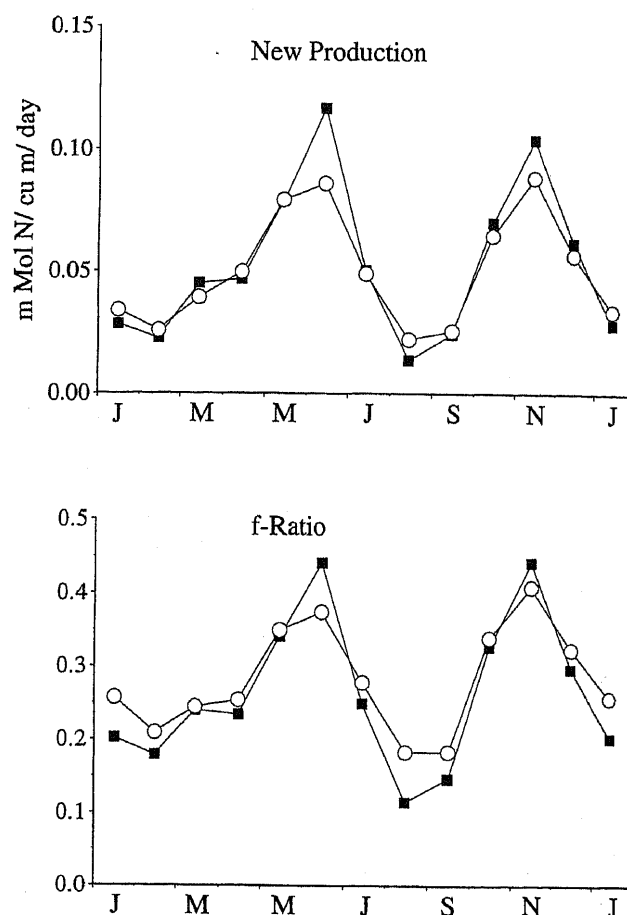


Figure 4. Seasonal variation of new production and f-ratio.

The zooplankton debris and sediment flux given in figure 5 show the significant role of the former in exporting nitrogen and also carbon. It is noted that the former includes the grazing by higher predators in this model. Both the versions show qualitatively the same behaviour.

Primary production F_p ($\text{m Mol N/m}^3/\text{day}$) correlates well with chlorophyll C (mg/m^3) and sediment flux F_s ($\text{mmol N/m}^3/\text{day}$) as shown in the scatter plot in figure 6. The correlations are given by

$$C = aF_p + b$$

$$F_s = cF_p + d$$

where a , b , c and d have values (0.013, 0.067, 0.001, 0.00099) and (0.006, 0.128, 0.002, -0.0005) in appropriate units in the non-switching and switching versions respectively, and the corresponding correlation coefficients are (0.95, 0.92) and (0.90, 0.92). Clearly, this simulation provides a partial theoretical basis for using empirical correlations to estimate primary production from satellite measurements of chlorophyll and sediment trap measurements. If the values of these coefficients are relatively insensitive to location and interannual variability, the use of such correlations would be justified.

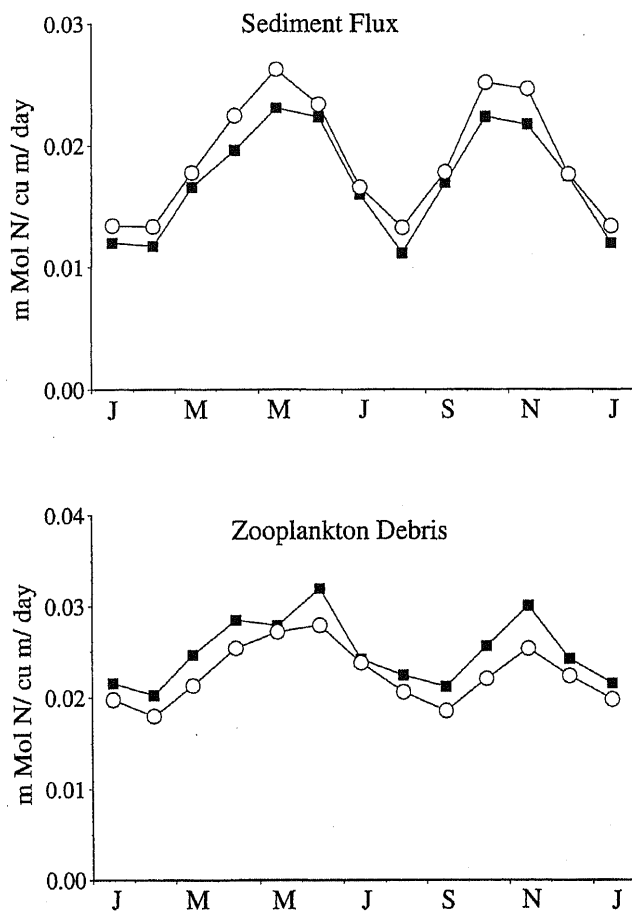


Figure 5. Seasonal variation of zooplankton debris and sediment flux.

It is observed that the function $h^+(t)$, which is equal to the rate of change of the mixed layer depth when it is deepening, is rather sensitive to the finite difference formula used in calculating the derivative. It consequently affects the nitrate input and chlorophyll quite a bit. The results shown are for the central difference formula. It is also noted that the use of monthly averages of mixed layer depth and the neglect of diurnal variation amounts to filtering of the input. While such a process may

not have significant effects in a linear system, it is unlikely to be so in the present system as it is nonlinear.

It is of interest to examine the balance of total nitrogen (N_t) in biota, in dissolved and particulate form in the mixed layer. It follows from the model that N_t is governed by the following relation.

$$\begin{aligned} \frac{dN_t}{dt} = & \frac{(m + h^+(t))}{M} (N_0 - N_n) \\ & - \frac{(m + h^+(t))}{M} (N_t - N_n - Z) \\ & - \left(\frac{h(t)}{M} + \Omega\mu_5 \right) Z - \frac{V}{M} D, \end{aligned}$$

where $N_t = P + Z + B + D + N_n + N_r + N_d$.

The first term on the right represents influx of nitrate into the mixed layer by diffusion and entrainment. The remaining terms represent efflux of all components other than nitrate.

A common assumption in several model studies is that there is equilibrium of total nitrogen in the mixed layer and a balance between nitrate input from below and nitrogen efflux in the form of detritus, zooplankton debris and various other forms of nitrogen. Figure 7 shows how the nitrate flux given by the first term and the efflux given by the rest of the terms in the above equation vary seasonally. In particular, it shows that the assumption of balance between the two is only approximately true, relative errors being larger in lean periods. Again, both the versions have qualitatively similar behaviour.

Turbulent mixing in the mixed layer assures vertical thermal homogeneity as the mean temperature is practically constant in the vertical direction. But it is not sufficiently strong to counteract the effects of radiation which decreases with depth and of the supplies of nitrate which increases with depth as shown by numerous observations (e.g., JGOFS cruises). While the present model assumes vertically homogeneous biological and biochemical processes, it is not a serious limitation as the present exercise is

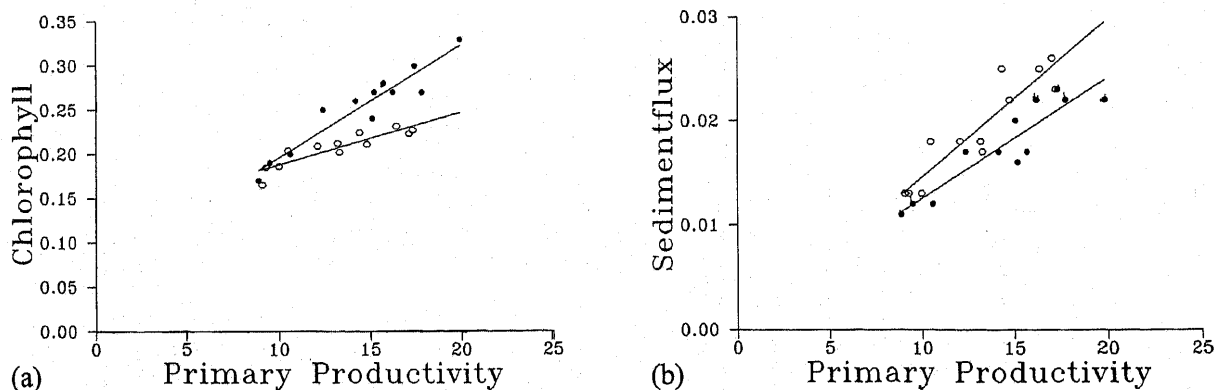


Figure 6. Scatter plots of chlorophyll, sediment flux with primary production.

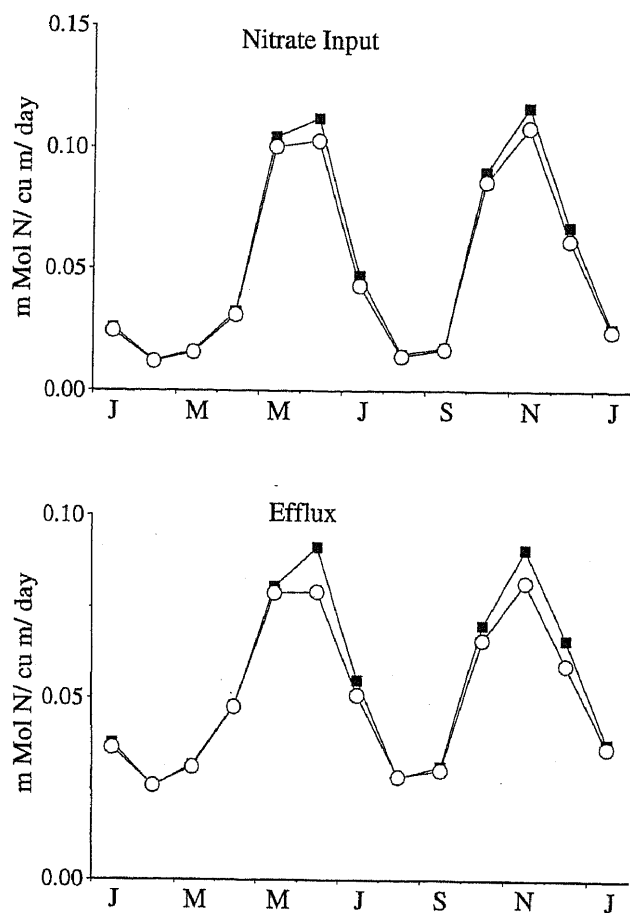


Figure 7. Nitrate input and nitrogen efflux due to all other causes.

intended primarily to serve as a calibration step. When the calibrated biological model is coupled to a physical oceanographic model, the vertical structure will be automatically captured.

6. Concluding remarks

It has been shown that it is possible to carry out the first stage of calibration of the ecosystem model, which is termed as macrocalibration, for the Arabian Sea despite acute sparsity of data.

It has been also shown that the switching and non-switching versions of the model with the same parameter calibration give qualitatively similar behaviour for the ecosystem, except that variations are somewhat muted in the switching version.

The present simulations have shown that the zooplankton biomass can dominate the biota in the tropical seas, unlike what is observed in temperate seas.

Some aspects of the model need further examination. For example, the significant reduction in chlorophyll and primary productivity from February–March to April–May is not captured by either version for a large range of parameters (tables 3 and

5). If this variation is not due to interannual variability, some detailed investigation is needed to determine whether the model structure needs modification.

Acknowledgements

The authors gratefully acknowledge the grant from the Department of Ocean Development under MAR-SIS and JGOFS programmes which made this work possible. We thank Prof. S Krishnaswami, PRL, Ahmedabad and Prof. M J R Fasham for their encouragement and useful discussions. We also thank SCOR for sponsoring the first author to attend the JGOFS Workshop on models of carbon cycle in the upper ocean and the participants of this workshop for giving useful inputs. Finally, the authors thank the referees for their comments which have resulted in significant improvement of the manuscript.

APPENDIX I

The following list gives many of the contemporary models. This information was made available at the International JGOFS meeting at Toulouse, France during November 1995.

Contemporary models	Components of the ecosystem model
David Antoine ¹	P, 2C.
K L Denmann ²	P, Z, N.
Scott Doney ³	P, Z, NO ₃ , D.
George Hurtt ⁴	P, NO ₃ , NH ₄ , R.
Dennis McGillicuddy ⁵	P, Z, NO ₃ , NH ₄ , Nexport (at bottom).
Uli Wolf ⁶	P, Z, D, Pellets, NO ₃ , NH ₄ .
Geoff Evans, Helge Drange ⁷ , Sharada	P, Z, B, D, NO ₃ , NH ₄ , DON (FDM type).
Veronique Garcon ⁸	P, Z, NO ₃ , SmallD, LargeD, Refrac DON, Labile DON.
Pascal Prunet ⁹	P, Micro Z, Meso Z, B, NH ₄ , NO ₃ , VSD, SD, LD, 2C, DO.
Aoki ¹⁰	P, Z, B, D, NO ₃ , NO ₂ , NH ₄ , PO ₄ , Labile DON, 2C, DO.
Diana Ruiz-Pino ¹¹	Nano P, Micro P, Micro Z, Meso Z, B, SD, LD, Si, DON/DOC, NH ₄ , NO ₃ .
Thomas Anderson ¹²	P, Z, B, D(N), D(C), DON, DOC, DIC, NH ₄ , NO ₃ .

APPENDIX II

Equations of the model

$$\begin{aligned}
\frac{dP}{dt} &= P \left[(1 - \gamma_1)\sigma - \mu_1 - G_1Z - \frac{m + h^+(t)}{M} \right], \\
\frac{dZ}{dt} &= Z \left[\beta_1 G_1 + \beta_2 G_2 B + \beta_3 G_3 D - (\mu_2 + \mu_5) - \frac{h(t)}{M} \right], \\
\frac{dB}{dt} &= B \left[-G_2 Z + U_1 + U_2 - \mu_3 - \frac{m + h^+(t)}{M} \right], \\
\frac{dD}{dt} &= -\mu_4 D + (1 - \beta_1)G_1 Z P + (1 - \beta_2)G_2 Z B \\
&\quad - \beta_3 G_3 Z D + \mu_1 P - \frac{m + h^+(t) + V}{M} D, \\
\frac{dN_n}{dt} &= -JQ_1 P + \frac{m + h^+(t)}{M} (N_0 - N_n), \\
\frac{dN_r}{dt} &= -JQ_2 P + U_2 B + \mu_3 B + [\varepsilon\mu_2 + (1 - \Omega)\mu_5]Z \\
&\quad - \frac{m + h^+(t)}{M} N_r, \\
\frac{dN_d}{dt} &= \mu_4 D + \gamma_1 JQP - U_1 B + (1 - \varepsilon)\mu_2 Z \\
&\quad - \frac{m + h^+(t)}{M} N_d,
\end{aligned}$$

where P , Z and B are phytoplankton, zooplankton and bacteria in mMol N/m^3 , D , N_n , N_r and N_d are

¹Antoine D and Morel A 1996 Oceanic primary production 1. Adaptation of a spectral light-photosynthesis model in view of application to satellite chlorophyll observations; *Global geochemical cycles* 10 43–55

²Denmann K L 1995 Biological-physical interactions in the upper ocean: The role of vertical and small scale transport processes; *Ann. Rev. Fluid Mech.* 27 225–255

³Doney S C, Glover D M and Najjar R G A new coupled, one-dimensional biological model for the upper ocean: Applications to the JGOFS BATS site; Personal communication.

⁴Hurt G C and Armstrong R A A pelagic ecosystem model calibrated with BATS data; Personal communication.

⁵McGillcuddy D Jr., Robinson A R and McCarthy J J 1995 Coupled physical and biological modelling of the spring bloom in the north Atlantic (II): Three dimensional bloom and post-bloom processes; *Deep Sea Res.* 42 1359–1398

⁶Uli Wolf, Personal communication.

⁷Drange H 1994 An isopycnic coordinate carbon cycle model for the north Atlantic; *Technical Report* No. 93, (Norway: The Nansen Environmental and Remote Sensing Center).

⁸Dadou I, Garcon V, Anderson V, Flierl G R and Davis C S, Impact of the north equatorial current meandering on a pelagic ecosystem: A modelling approach; Personal communication.

⁹Pascal Prunet P, Minster J F, Ruiz-Pino D and Dadou I 1996 Assimilation of surface data in a one-dimensional model of the surface ocean (1) Method and preliminary results; *Global biogeo-chemical cycles* 10 111–138

¹⁰Aoki, Personal communication.

¹¹Ruiz-Pino D, Personal communication.

¹²Anderson T 1992 Modelling the influence of food C:N ratio, and respiration on growth and nitrogen excretion in marine zooplankton and bacteria; *J. Plankton Res.* 14 1645–1671

detritus, nitrate, ammonium and dissolved organic nitrogen mMol N/m^3 , t is time in units of day. The parameters are defined subsequently. The units and values are given in brackets.

In the above,

$$\frac{dM}{dt} = h(t), \quad h^+(t) = \max(0, h(t)),$$

$$J = \frac{2}{M} \int_0^\tau \int_0^M F(I_0(t) \exp[-(k_w + k_c P)z]) dz dt,$$

$$F(I) = \frac{V_p \alpha I}{(V_p^2 + \alpha^2 I^2)^{1/2}},$$

$$Q = Q_1 + Q_2 = \frac{N_n e^{-\psi N_r}}{K_1 + N_n} + \frac{N_r}{K_2 + N_r},$$

$$\sigma = JQ,$$

$$F = p_1 P + p_2 B + p_3 D.$$

Non-switching version

$$G_1 = g \frac{p_1}{K_3 + F}$$

$$G_2 = g \frac{p_2}{K_3 + F}$$

$$G_3 = g \frac{p_3}{K_3 + F}$$

$$S = \min(N_r, \eta N_d),$$

$$U_1 = \frac{V_b N_d}{K_4 + S + N_d},$$

$$U_2 = \frac{V_b S}{K_4 + S + N_d},$$

Switching version

$$G_1 = g \frac{p_1 P}{K_3 F + p_1 P^2 + p_2 B^2 + p_3 D^2},$$

$$G_2 = g \frac{p_2 B}{K_3 F + p_1 P^2 + p_2 B^2 + p_3 D^2},$$

$$G_3 = g \frac{p_3 D}{K_3 F + p_1 P^2 + p_2 B^2 + p_3 D^2},$$

MODEL PARAMETERS AND FORCING FUNCTIONS

Related to physical oceanography

Mixed layer depth, M (m).

PAR immediately below the surface water, I_0 (W/m^2).

Light attenuation coefficient due to water, k_w (0.04 m^{-1}).

Diffusion/Mixing coefficient, m (m/day).

Related to phytoplankton

Phytoplankton maximum growth rate, V_p (2.9/day).

Initial slope of P-I curve, α ($0.025 \text{ (W m}^{-2})^{-1} \text{ d}^{-1}$).

Half-saturation for phytoplankton nitrate uptake, K_1 ($0.5 \text{ m Mol N/m}^{-3}$).

Half-saturation for phytoplankton ammonium uptake, K_2 ($0.5 \text{ m Mol N/m}^{-3}$).

Phytoplankton specific mortality rate, μ_1 (0.09/day).

Light attenuation by phytoplankton, k_c ($0.03 \text{ m}^2 (\text{m Mol N})^{-1}$).

Phytoplankton exudation fraction, γ_1 (0.05).

Ammonium inhibition parameter, ψ ($1.5 (\text{m Mol N})^{-1}$).

Subsurface nitrate concentration, N_0 (m Mol N/m^3).

Related to zooplankton

Zooplankton asymptotic grazing rate, g (/day).

Zooplankton assimilation efficiency, $\beta_1, \beta_2, \beta_3$ (0.75, 0.75, 0.75).

Zooplankton preferences, p_1, p_2, p_3 .

Zooplankton specific excretion rate, μ_2 (0.1/day).

Zooplankton specific mortality rate, μ_5 (0.05/day).

Zooplankton half-saturation for ingestion, K_3 (1/day).

Detrital fraction zooplankton mortality, Ω (0.33).

Ammonium fraction of zooplankton excretion, ε (0.75).

Related to bacteria

Bacterial maximum growth rate, V_b (2/day).

Bacterial specific excretion rate, μ_3 (0.05/day).

Bacterial half-saturation for uptake, K_4 ($0.5 \text{ m Mol N/m}^{-3}$).

Ammonium/DON uptake ratio, η (0.6).

Related to detritus

Detrital breakdown rate, μ_4 (0.05/day).

Detrital sinking rate, V (m/day).

References

- Banase K 1994 On the coupling of hydrography, phytoplankton, zooplankton and settling organic particles offshore in the Arabian Sea; In *Biogeochemistry of the Arabian Sea*, Proc. Earth Planet. Sci. (ed) D Lal, 103 27–64
- Evans G T and Parlow J S 1985 A model of annual plankton cycles; *Biological Oceanography* 3 327–427
- Fasham M J R, Ducklow H W and McKelvie S M 1990 A nitrogen-based model of the plankton dynamics in the oceanic mixed layer; *J. Mar. Res.* 48 591–639
- Fasham M J R, Sarmiento J C, Slater R D, Ducklow H W and Williams R 1993 A seasonal three-dimensional ecosystem model of nitrogen cycling in the north Atlantic euphotic zone: A comparison of the model results with observation from Bermuda station "S" and OWS "India"; *Global Biogeochemical Cycles* 7 379–415
- Foley J A, Taylor K E and Ghan S J 1991 Planktonic dimethylsulphide and cloud albedo: An estimate of the feedback response; *Climatic Change* 18 1–15
- Frost B W 1987 Grazing control of phytoplankton stock in the open sub-arctic Pacific Ocean: A model assessing the role of mesozooplankton particularly the large calanoid copepods neocalanus; *Mar. Ecol. Ser.* 39 49–68
- Lal D 1994 Biogeochemistry of the Arabian Sea: Present information and gaps; *Biogeochemistry of the Arabian Sea Proc. Earth Planet. Sci.* (ed) D Lal 103 1–7
- Levin S A 1980 Population dynamics and community structure in heterogeneous environments; *Mathematics Biology* 295–320
- Rao R R, Molinari R L and Festa J F 1991 Surface meteorological and near-surface oceanographic atlas of the tropical Indian Ocean; *NOAA Technical Memorandum ERL AOML-69*
- Riley G A, Stommel H and Burpus D P 1949 Qualitative ecology of the plankton of the western north Atlantic; *Bull. Bingham Ocean. Collect.* 112 1–169
- Sarmiento J L, Slater R D, Fasham M J R, Ducklow H W, Toggweiler J R and Evans G T 1993 A seasonal three-dimensional ecosystem model of nitrogen cycling in the north Atlantic euphotic zone; *Global Biogeochemical Cycles* 7 417–450
- Sathyendranath S, Gouveia A D, Shetye S R, Ravindran P and Platt T 1991 Biological control of surface temperature in the Arabian Sea; *Nature (London)* 349 54–56
- Sathyendranath S and Platt T 1994 New production and mixed-layer physics; In *Biogeochemistry of the Arabian Sea*, (ed) D Lal Proc. Indian Acad. Sci. (Earth Planet. Sci.) 103 79–90
- Shetye S R, Gouveia A D and Shenoi S S C 1994 Circulation and water masses of the Arabian Sea; In *Biogeochemistry of the Arabian sea*, Proc. Earth Planet. Sci. (ed) D Lal 103 9–26
- Steele J H 1974 *The structure of marine ecosystems*, (Oxford: Blackwell)
- Steele J H and Frost B W 1977 The structure of plankton communities; *Philos Trans. R. Soc. London* B280 485–534
- Taylor A H and Joint I 1990 A steady-state analysis of the 'microbial loop' in stratified systems; *Mar. Ecol. Prog. Ser.* 59 1–17
- U S Global Ocean Ecosystem Dynamics, 1993 Report No. 9
- Wroblewski J S, Sarmiento J L and Fliel G R 1988 An ocean basin scale model of plankton dynamics in the north Atlantic. Solutions for the climatological oceanographic condition in May; *Global Biogeochemical Cycles* 2 199–218
- Wroblewski J S, Richman J G and Mellor G L 1989 Optimal wind conditions for the survival of larval northern anchovy, *Engraulis mordax*: A modelling investigation; *Fishery Bulletin U.S.* 87 387–395
- Yajnik K S and Sharada M K 1992 Dynamics of a basic phytoplankton model: In *Oceanography of the Indian Ocean* (ed) B N D Desai, Publ. International Book House 91–98